Features of The Magnetic Field of a Rectangular Combined Function Bending Magnet

C. S. Hwang[a),b)], C. H. Chang[a)], G. J. Hwang[d)], T. M. Uen[b)] and P. K. Tseng[a),c)]

[a)]Synchrotron Radiation Research Center, Hsinchu Science-Based Industrial Park, Hsinchu 30077, Taiwan
[b)]Department of Electrophysics, National Chiao Tung University, Hsinchu, Taiwan
[c)]Department of Physics, National Taiwan University, Taipei , Taiwan
[d)]Department of Power Mechanical Engineering, National Tsing Hua University, Hsinchu, Taiwan

***Abstract*—Magnetic field features of the combined function bending magnet with dipole and quadrupole field components are essential for the successful operation of the electron beam trajectory. These fields also dominate the photon beam quality. The vertical magnetic field $B_y(x,y)$ calculation is performed by a computer code "MAGNET" at the magnet center ($s=0$). Those results are compared with the 2-D field measurement by the Hall probe mapping system. Also detailed survey has been made of the harmonic field strength and the main features of the fundamental integrated strength, effective length, magnetic symmetry, tilt of the pole face, offset of the field center and the fringe field. The end shims that compensate for the strong end negative sextupole field to increase the good field region for the entire integrated strength are discussed. An important physical feature of this combined function bending magnet is the constant ratio of dipole and quadrupole strength $\int Bds/\int Gds$ which is expressed as a function of excitation current in the energy range 0.6 to 1.5 GeV.**

I. Introduction

The combined function bending magnet is operated at a nominal energy of 1.3 GeV (the excitation current is about 940 A). However, it may be upgraded to 1.5 GeV in the near future, and the magnetic field quality must therefore be surveyed at this energy. The magnet is a combined function laminated dipole magnet [1], that is curved ($\theta=\pm 10^o$) with rectangular edges, subsequently producing an integral magnetic field 1.5137 T·m and integral gradient strength 1.957 T at the nominal energy 1.3 GeV. The magnet length is 1.22 m and the nominal curvature radius ρ is 3.495 m. The bending angle θ is equal to 20^o. The design value for the beam dynamics of the ratio between the dipole and quadrupole strength is -0.7735. The Hall probe mapping system [2], [3] was used to measure the magnetic field; in this manner, the analytical methods [4] and alignment procedure [5] for this mapping system were developed. As the demands of beam dynamics lead to the use of the curvilinear coordinate x-y-s system in a bending magnet, the same x-y-s system should be selected to map the magnetic field distribution.

Finally, an important characteristic of the combined function bending magnet is the ratio of $\int Bds/\int Gds$. The deviation of this ratio with varied excitation currents is measured. This value will limit the energy range of operation. Measurements with shims for varied excitation current are made to increase the good field region at 1.3 and 1.5 GeV. Fig. 1 shows the locations of shims and the fringe field behavior is discussed. Results obtained from these measurements and analysis demonstrate that the combined function bending magnet is satisfactory for operation in the energy range from 0.6 to 1.5 GeV.

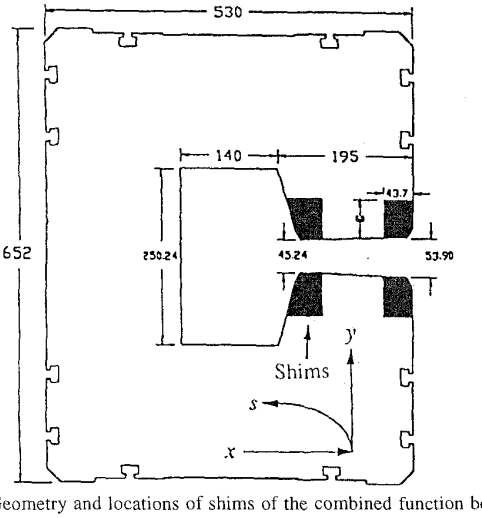

Fig. 1. Geometry and locations of shims of the combined function bending magnet.

II. Mapping Trajectory And Definition

A rectangular magnet differs from a sector one. Therefore, for this bending magnet, the mapping trajectory is along the curvilinear trajectory x-y-s [6]. On the midplane, the mapping trajectory follows three different trajectory directions. In the region of $-10^o \le \theta \le 10^o$ (inside the magnet), the Hall probe follows either the arc of a circle in the longitudinal s-axis or the radial displacement $\rho \pm r$ perpendicular to the arc of circle curve trajectory s-axis. In the range of $|\theta| \ge 10^o$ (outside the magnet region), in which θ is kept constant at 10^o, the Hall probe follows either a radial displacement ρ perpendicular to the curve trajectory s-axis or along a slop straight line which is tangential to the arc of the circle to measure the fringe field distribution. Where θ is the angle between x-axis and radial direction. The exact center $(0,0,0)$ of the magnet would determine the proper reference trajectory.

The vertical field $By(x)$ are expanded at $s=0$ (where $r=x$) by means of equation (1) via least-square fitting; the

0018-9464/96$05.00 © 1996 IEEE

harmonic field of normal components at the magnetic center is subsequently obtained.

$$B_y(x) = B + G\,x + S\,x^2 + O\,x^3 + D\,x^4 + \text{----} \quad (1)$$

If the harmonic field is integrated along a longitudinal direction, the vertical integral field $\int B_y(x,s)ds$ can be expressed as

$$\int B_y(x,s)ds = \int Bds + \int Gds\,x + \int Sds\,x^2 + \int Ods\,x^3 + \int Dds\,x^4 + \text{----} \quad (2)$$

Therefore, if one needs to know the good field region or the field quality, analysis should be performed to plot the distribution of field deviation as a function of the horizontal transverse x-axis. The field deviation of both the center ($y=s=0$) and integral field ($y=0$) is defined as

$$\Delta B/B = [B_y(x) - (B + G\,x)] / (B + G\,x), \quad (3)$$

$$(\Delta\int Bds)/\int Bds = [\int B_y(x,s)ds - (\int Bds + \int Gds\,x)] / (\int Bds + \int Gds\,x). \quad (4)$$

To analyze the center offset of the magnetic field on the longitudinal s-axis, the actual pole face shape is plotted by calculating the effective length. The half effective length of the magnet upstream and downstream is defined as

$$L_u = \int_{-\infty}^{0} B_y(x,s)ds/B(0,0), \quad (5)$$

$$L_d = \int_{0}^{\infty} B_y(x,s)ds/B(0,0). \quad (6)$$

The magnetic field center offset on the longitudinal direction is defined as

$$L_{offset} = (L_u - L_d)/2. \quad (7)$$

III. Measurement And Analysis Result

The 2-D design of the vertical field $B_y(x,y)$ on excitation current 920 A at magnet center (s=0) was calculated by the "MAGNET" code [7]. This result was shown in Table I. The field $B_y(x,y)$ was also measured by the Hall probe mapping system. These data were inserted into equation (1) via the least-square fitting method to obtain the fundamental and higher multipole strength. Fig. 2 shows the higher multipole error $\Delta B/B$ of measurement and design results at different excitation current on the magnet center $y=s=0$. This result shows that the field behavior after magnet fabrication closed corresponds to the design results. The good field range $\Delta B/B$ has been within the specification of $\pm 2\times10^{-4}$ in the range of transverse direction $-12 \le x \le 12$ mm. Althought the good field region of $\Delta B/B$ at 1195 A (1.5 GeV) is much shorter than the other current, but it is also close to the specification.

The end shims were made to increase the good field region such that the photon beam quality is markedly improved. According to Fig. 3, adding two pieces of lamination (lamination of thickness 1.5 mm) on each side of the magnet (see Fig. 1) produces the optimum field quality at nominal excitation current 940 A (1.3 GeV). After adding the 2 shims, the sextupole field was compensated at the magnet edges (see Fig. 6) and the good field region for the integrated strength was also much wider than before. Table I presents the main harmonic and the higher multipole integrated strength, which indicates that the multipole strengths are all within tolerance. In Fig. 4, the good field region without shim at 1.5 GeV is out of the specification. However, the five pieces of shims were added and the optimum field quality was obtained. The fundamental and higher multipole field integral strength are also revealed in Table II, indicating that the multipole strengths are close tolerance with five pieces of shims compensating for the field saturation behavior at the two edges of magnet.

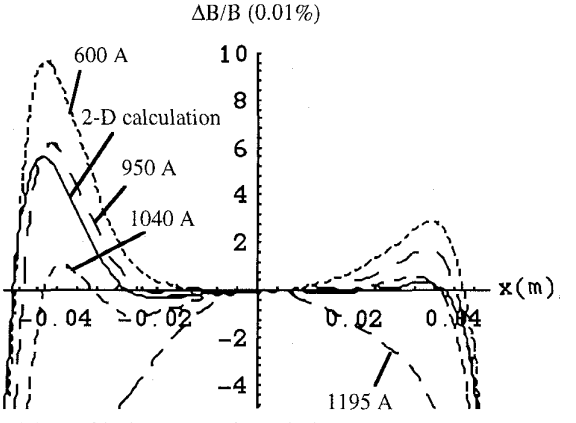

Fig. 2. Higher multipole error of a 2-D calculation and measurement results on the magnetic center at varied excitation current.

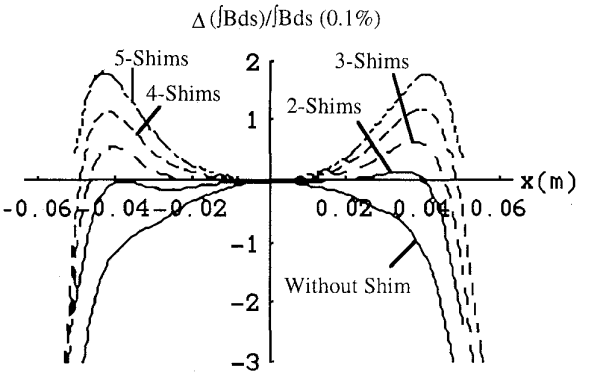

Fig. 3. Deviation of higher multipole integral strength for ∫Bds with and without shims at nominal excitation current 940 A (1.3 GeV).

The sextupole strength at 1.3 and 1.5 GeV is strong at the magnet edges but weak in the center. The strong sextupole field at the two edges is produced from the fringe field that creates a strong saturation behavior. The sextupole field

behavior, at the magnet edge, with and without shims at 1.3 and 1.5 GeV are shown in Fig. 5 and 6 individually. A comparison of these figures reveals that the sextupole strength at 1.5 GeV is stronger than 1.3 GeV either in the center region or at magnet edge. The strong sextupole field can be compensated by adding the end shims to increase the good field region. Table II and Fig. 4 verify that this magnet can be operated at 1.5 GeV. Hence, SRRC has decided to upgrade the 1.3 GeV machine to 1.5 GeV in the near future.

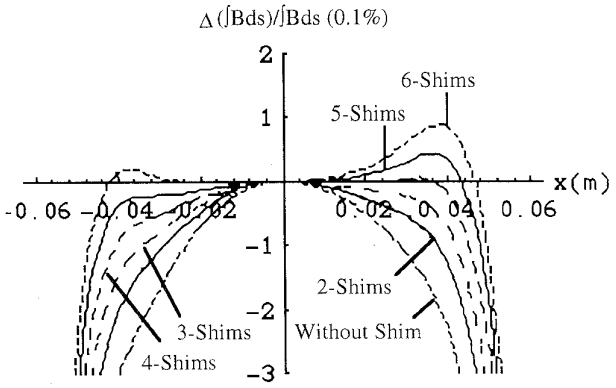

Fig. 4. Deviation of higher multipole integral strength ∫Bds with and without shims at the excitation current 1195 A (1.5 GeV).

TABLE I
HARMONIC FIELD STRENGTH OF DESIGN AND MEASUREMENT AT NOMINAL CURRENT 940 A WITH 2 SHIMS (AT 1.3 GeV).

		2-D calculation	Measurement	Tolerance††
B(0)	(T)	1.2409 (1.2407†)	1.2400	----
G(0)	(T/m)	-1.7108 (-1.604†)	-1.7161	----
S(0)	(T/m^2)	-0.007	-0.027	----
O(0)	(T/m^3)	3.03	4.88	----
D(0)	(T/m^4)	73.9	-105.7	----
∫Bds	(T·m)	----	1.51521	----
∫Gds	(T)	----	-1.9736	----
∫Sds	(T/m)	----	-0.216 (-1.69*)	0.89±0.27
∫Ods	(T/m^2)	----	12.5 (15*)	±14.5
∫Dds	(T/m^3)	----	-43 (-230*)	-258±474

* Without shims
† Specification value
†† The error tolerance specified is within the good field region.

The center offset between magnetic field and magnet mechanical must be found in the longitudinal directions. Moreover the field center is determined by the half effective length and is defined as equation (7). Fig. 7 indicates a -0.23 mm of center offset in the longitudinal direction. Hence, the alignment should depend on this center offset to install a dipole magnet on the storage ring. Depending on the definition of half effective length on the magnet upstream and downstream, the half effective length is shown in Fig. 7 as a function of horizontal transverse x-axis, revealing that the pole face at the two edges of the magnet is bent but symmetric.

For a good magnet design, the ratio value of ∫Bds/∫Gds is as close to -0.7735 as possible. Fig. 8 indicates that the integral field normalization of *[(∫Bds/∫Gds)+0.7735]/0.7735*

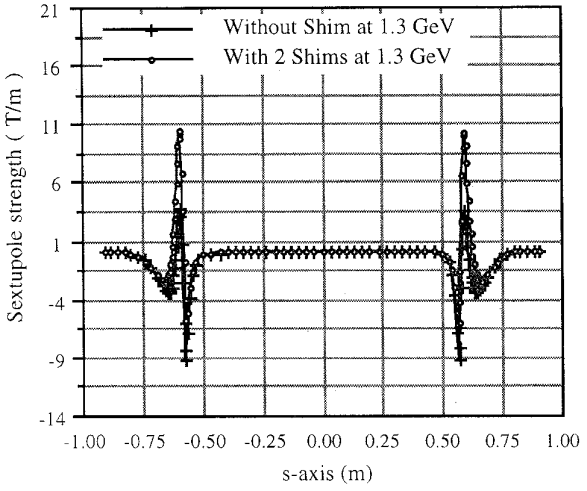

Fig. 5. Distribution of sextupole field strength along the longitudinal direction with and without shims at 1.3 GeV.

TABLE II
HARMONIC FIELD STRENGTH WITH AND WITHOUT SHIMS, WITH MEASUREMENT AT CURRENT 1195 A (AT 1.5 GeV).

		With Shims	Without Shims	Tolerance
∫Bds	(T·m)	1.7440*	1.7445	----
∫Gds	(T)	-2.248	-2.242	----
∫Sds	(T/m)	-0.198	-2.49	0.89± 0.27
∫Ods	(T/m^2)	28.5	30.9	± 14.5
∫Dds	(T/m^3)	20	-534	-258± 474

* B(0) = 1.4360 T and effective length is 1.2144 m at 1.5 GeV.

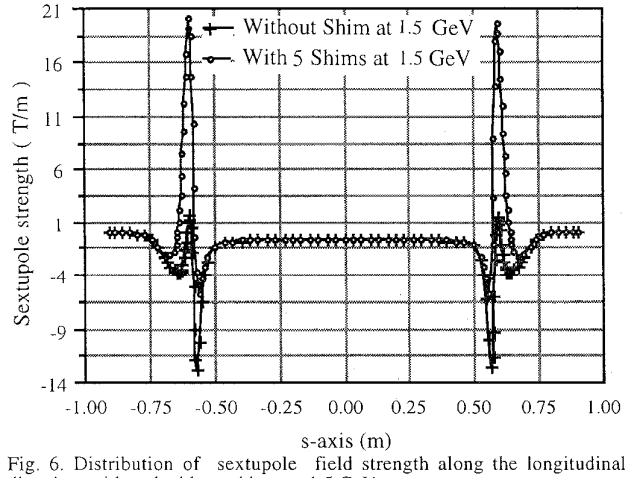

Fig. 6. Distribution of sextupole field strength along the longitudinal direction with and without shims at 1.5 GeV.

between maximum and minimum current is within 3.0%, the integral field normalization is 0.6% larger than the exact value -0.7735 at 1.3 GeV and -0.75% lower than the value at 1.5 GeV. Therefore, the small ratio difference is sufficient to operate at 1.5 and 1.3 GeV.

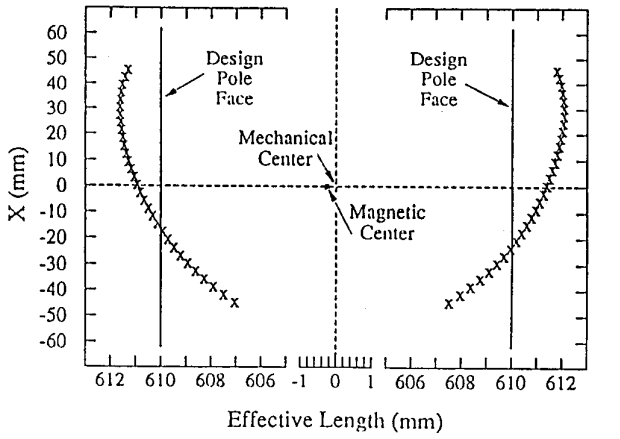

Fig. 7. Half the effective length distribution as a function of transverse x-axis on the two sides of the magnet. The ideal pole face is located at the effective length of 610 mm.

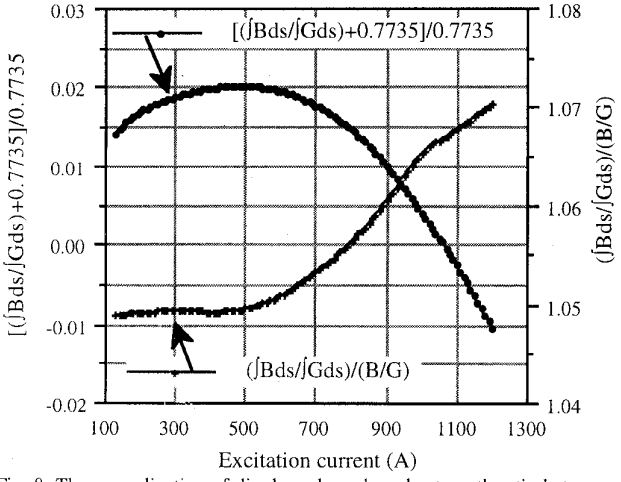

Fig. 8. The normalization of dipole and quadrupole strength ratio between the integral field and the center field at different excitation current.

For an actual combined function magnet, the ratio value of integral field $\int Bds/\int Gds$ may be different from the center field B/G at either nominal or different excitation current. Therefore, the experimental formula should be known to design a good approximation ratio of ∫Bds/∫Gds. Fig. 8 also reveals that the ratio between integral field and center field is a function of different excitation currents and that the ratio of integral field is larger than the center field ratio. Therefore when designing the magnet, the field ratio of B/G must be adjusted to be around 1.065 smaller than the design value -0.7735 to match the energy range of 1.3 to 1.5 GeV. Consequently, the integral field ratio of $\int Bds/\int Gds$ will be close to exact value of -0.7735.

IV. Conclusion

When the 2-D calculation code is used to design a combined function bending magnet, the actual ratio of the center field of dipole and quadrupole strength B/G should be 1.065 smaller than the exact value at nominal energy to match the specification of integral field ratio value -0.7735. This is since the actual behavior of the integral field ratio is higher than the center field ratio 1.065 at 1.3 GeV. The curve of $(\int Bds/\int Gds)/(B/G)$ as a function of excitation current can be treated as the experimental formula for designing the combined function bending magnet. At the same time, the nominal ratio value -0.7735 is one of the essential factor to determine the features of the other magnets for mass production. Because the nominal ratio $\int Bds/\int Gds$ is a important parameter of the combined function bending magnet for the beam dynamics demand.

After the 2 and 5 shims were added at the two edges of the magnet, the strong negative sextupole strength is compensated and the field quality is therefore sufficient to operate at 1.3 and 1.5 GeV individually. Although the total effective length with 2 shims is 2 mm longer than the specification 1.22 m at 1.3 GeV, and with 5 shims is 5.6 mm shorter than specification at 1.5 GeV. However, this does not affect the electron beam closed orbit [8].

Acknowledgments

The authors are indebted to Dr. C. S. Hsue, C. C. Kuo and Mr. J. C. Lee of the Beam Dynamics Group for discussing the required analysis of dipole magnetic mapping data, and Mr. T. C. Fan, F. Y. Lin, Shuting Yeh for their help in treating and measuring data.

References

[1] C. H. Chang, H. C. Liu and G. J. Hwang, " Design and Performance of the Dipole Magnet For The SRRC Storage Ring ," *Proceedings of the 1993 Particle Accelerator Conference*, vol. 4, pp. 2886, 1993.

[2] C. S. Hwang, W. C. Chou, J. H. Huang, M. Y. Lin, Tzuchu Chang, P. K. Tseng, " High precision automatic magnetic field mapping system for the dipole magnet ," *11-th International Conference on Magnet Technology*, pp. 291, 1989.

[3] C. S. Hwang, F. Y. Lin, G. J. Jan, P. K. Tseng, " High-precision harmonic magnetic-field measurement and analysis using a fixed angle Hall probe," *Rev. Sci. Instrum.* vol. 65 , No. 8, pp. 2548 , August 1994.

[4] Poh-Kun Tseng, Ching-Shiang Hwang, " The analysis methods of Hall probe mapping system for the combined function dipole magnet," *XVth International Conference On High Energy Accelerators*, vol.1, pp. 598- 601, 1992.

[5] C. S. Hwang , P. K. Tseng, W. C. Chou , J. H. Huang , " The Alignment procedure between the Hall probe measurement system and the TBA dipole magnet, " *SRRC/ MM/ IM/ 90-01.*

[6] C. S. Hwang, P. K. Tseng,W. C. Chou, J. H. Huang,"The Procedure for Mapping Trajectory and Analysis Of TBA Dipole Magnet, "*SRRC /MM /IM/90-02.*

[7] Ch. Iselin, " Two-dimensional magnetic fields including saturation (MAGNET)," *CERN computer center program library, long write up T600 , Geneva, 1977.*

[8] J. C. Lin, C. S. Hsue, " The Problem Raised from The Lengthening of Dipole Magnet Effect and its possible solution, " *SRRC/BD/IM/91-19, 1991.*